processes

MDPI

Article

The Pore Structure Multifractal Evolution of Vibration-Affected Tectonic Coal and the Gas Diffusion Response Characteristics

Maoliang Shen [1,2,*], Zhonggang Huo [1,2], Longyong Shu [1,2], Qixian Li [1,2,*], Pengxin Zhang [1,2] and Weihua Wang [1,2]

[1] China Coal Research Institute, Beijing 100013, China; huozhonggang@sohu.com (Z.H.); slyccri@163.com (L.S.); zpx3263@163.com (P.Z.); wh1987_wang@163.com (W.W.)
[2] State Key Laboratory of Coal Mine Disaster Prevention and Control, Beijing 100013, China
* Correspondence: shensml2010@163.com (M.S.); liqixian0219@163.com (Q.L.)

Abstract: Vibrations caused by downhole operations often induce coal and gas outburst accidents in tectonic zone coal seams. To clarify how vibration affects the pore structure, gas desorption, and diffusion capacity of tectonic coal, isothermal adsorption-desorption experiments under different vibration frequencies were carried out. In this study, high-pressure mercury intrusion experiments and low-pressure liquid nitrogen adsorption experiments were conducted to determine the pore structures of tectonic coal before and after vibration. The pore distribution of vibration-affected tectonic coal, including local concentration, heterogeneity, and connectivity, was analyzed using multifractal theory. Further, a correlation analysis was performed between the desorption diffusion characteristic parameters and the pore fractal characteristic parameters to derive the intrinsic relationship between the pore fractal evolution characteristics and the desorption diffusion characteristics. The results showed that the vibration increased the pore volume of the tectonic coal, and the pore volume increased as the vibration frequency increased in the 50 Hz range. The pore structure of the vibration-affected tectonic coal showed multifractal characteristics, and the multifractal parameters affected the gas desorption and diffusion capacity by reflecting the density, uniformity, and connectivity of the pore distribution in the coal. The increases in the desorption amount (Q), initial desorption velocity (V_0), initial diffusion coefficient (D_0), and initial effective diffusion coefficient (D_e) of the tectonic coal due to vibration indicated that the gas desorption and diffusion capacity of the tectonic coal were improved at the initial desorption stage. Q, V_0, D_0, and D_e had significant positive correlations with pore volume and the Hurst index, and V0, D0, and De had negative correlations with the Hausdorff dimension. To a certain extent, vibration reduced the local density regarding the pore distribution in the coal. As a result, the pore size distribution was more uniform, and the pore connectivity was improved, thereby enhancing the gas desorption and diffusion capacity of the coal.

Keywords: multifractal evolution; pore structure; vibration; gas diffusion; tectonic coal

check for updates

Citation: Shen, M.; Huo, Z.; Shu, L.; Li, Q.; Zhang, P.; Wang, W. The Pore Structure Multifractal Evolution of Vibration-Affected Tectonic Coal and the Gas Diffusion Response Characteristics. *Processes* **2024**, *12*, 1701. https://doi.org/10.3390/pr12081701

Academic Editor: Raymond Cecil Everson

Received: 30 July 2024
Revised: 10 August 2024
Accepted: 12 August 2024
Published: 14 August 2024

Copyright: © 2024 by the authors. Licensee MDPI, Basel, Switzerland. This article is an open access article distributed under the terms and conditions of the Creative Commons Attribution (CC BY) license (https://creativecommons.org/licenses/by/4.0/).

1. Introduction

China has extremely complex coal seam reserve conditions [1,2]. With the continuous increase in mining depth, the gas content and gas pressure of the working seam have gradually increased, and coal and gas outburst accidents still seriously threaten the safe production of coal mines [3–5]. Such coal and gas outburst accidents are often preceded by supporting, coal falling, drilling, blasting, coal cutting, and other on-site operations that can produce mechanical vibration. Studies have shown that the energy required for coal pulverization, gas desorption, and gas-solid mixture bursts is transmitted by the surrounding rock of the coal seam through vibration [6]. Therefore, vibration can be considered one of the main critical causes of coal and gas outburst accidents.

In the past 20 years, experts and scholars have extensively studied the effects of vibration on coal permeability, porosity, mechanical properties, and gas adsorption-desorption capacity, and some results have been achieved. Ren et al. [7,8] and Pan et al. [9] found that

vibration can alter the stress state of the coal mass, and the induced cracks in the coal mass have a certain softening effect on it. Song et al. [10,11] found through experiments and CT imaging that mechanical vibration is conducive to crack expansion and development in the coal mass, increasing its permeability. Ren et al. [12] and Wen et al. [13] studied the response characteristics of coal vibration induced by simple harmonic vibration, concluding that the mechanical parameters of coal determined its vibration response characteristics, and the peak values of the response parameters increased significantly when the excitation force frequency resonated with the natural frequency of the coal mass. Wei et al. [14,15] further explored the influence of low-frequency vibration on the permeability of coal samples, concluding that the permeability growth rate of the coal mass increased first and then decreased as the vibration frequency increased, and the permeability enhancement was greater near the resonance frequency. Li et al. [16] found that vibration can reduce the gas adsorption capacity of the coal mass and accelerate gas desorption. Meanwhile, their analysis from the perspective of fracture mechanics concluded that vibration caused unstable crack expansion and development in the coal mass, thus inducing bursts. Shen et al. [17,18] concluded that vibration could cause pore structure changes in the coal mass, which increased the gas diffusion path and reduced the diffusion resistance, thus promoting gas desorption in particulate coal.

Coal and gas outburst sites are typically characterized by the development of tectonic coal, with tectonic coal development at almost all outburst sites [19–21], i.e., the wide tectonic coal reserve plays a decisive role in the outburst [22]. The microstructure of the coal mass is closely related to its mechanical properties, and the yield and failure of the coal mass are the macroscopic manifestations of the evolution of microscopic pores and cracks [23]. At present, experts and scholars have conducted a series of studies on the differences in microstructure and physical properties of tectonic coal and primary coal. Previous research results showed that tectonic coal had significantly decreased pore compressibility due to tectonic deformation [24]. Compared with primary coal, tectonic coal has the characteristics of low mechanical strength, weak adhesion, and weak resistance to external stress disturbance, and its natural particles are smaller and more likely to break into small-particle coal powder [22,25]. Meanwhile, tectonic coal has more complex pore structure characteristics than primary coal, with more intensive pore development, a lower pore-throat ratio, and lower tortuosity than primary coal [26]. Tectonic coal has a strong gas adsorption-desorption capacity, and its initial gas desorption and diffusion capacity is greater than that of primary coal [27–29], leading to rapid gas desorption at the initial desorption stage and promoting the release of gas energy [4,30–32].

Despite the great progress in the research on how vibration influences the physical properties of the coal mass, the differences in pore structure and physical properties between primary coal and tectonic coal were not considered. Due to its low mechanical strength, easy pulverization, weak resistance to external stress disturbance, complex pore structure, and strong adsorption-desorption capacity, tectonic coal must exhibit different response characteristics from primary coal when subjected to vibration. Therefore, on the basis of previous studies, pore structure determination and gas desorption and diffusion experiments were conducted on vibration-affected tectonic coal in this research. The evolutionary characteristics of pore heterogeneity and connectivity in vibration-affected tectonic coal were analyzed using multifractal theory. A correlation analysis was performed between the pore structure characteristic parameters and the gas desorption and diffusion characteristic parameters to derive the pore fractal characteristics and gas desorption and diffusion response characteristics of the vibration-affected tectonic coal and the intrinsic connection between them. The research results can provide theoretical guidance for gas management and coal and gas outburst prevention in tectonic coal mines.

2. Methods and Theory

2.1. Coal Sample Selection and Preparation

In the experiment, tectonic coal was collected from the Wangxingzhuang Coal Mine (WXZ) in Henan and the Gaohe Coal Mine (GH) in Shanxi. The Wangxingzhuang Coal Mine is located in the Xinmi coalfield. Due to the influence of tectonic action in the coalfield area, the II_1 coal seam presents the characteristics of the development of tectonic coal in the whole coal seam. The WXZ coal sample collection site is located in the 15,021 working face of the II_1 coal seam. Structures such as faults, folds, and collapse columns were developed in the Gaohe coal mine field. The GH coal sample collection site is located in the structural area of the south wing roadway passing through the footwall of the F_3 fault. The freshly collected samples were sealed and transferred to the laboratory. After crushing, coal samples 1~3 mm in size were selected. The coal from each mine was divided into 3 even samples, 200 g each. The basic physical parameters of the coal sample are presented in Table 1.

Table 1. Basic coal sample physical parameters.

Coal Sample	Adsorption Constant		Industrial Analysis			TRD (g/m^3)	ARD (g/m^3)	φ (%)
	a (m^3/t)	b (MPa^{-1})	Mad (%)	Ad (%)	Vdaf (%)			
WXZ	26.32	2.74	0.88	7.73	13.81	1.43	1.38	3.19
GH	26.18	0.7184	0.28	4.97	11.84	1.41	1.37	2.84

2.2. Experimental Equipment and Processes

After the coal sample preparation, a MicroAutoPore IV type 9500 mercury piezometer and an ASAP type 2460 physical adsorption instrument were used to perform high-pressure mercury intrusion experiments and low-pressure liquid nitrogen adsorption experiments, thus characterizing the pore structure of the coal sample before vibration. In order to ensure the reliability of the test results, the instrument was calibrated using the standard samples provided by the instrument manufacturer before the high-pressure mercury injection experiment and the low-pressure liquid nitrogen adsorption experiment.

An MVGAD-I type vibration condition isothermal adsorption-desorption platform independently developed by our research team was used to perform isothermal gas adsorption-desorption experiments of coal under vibration, where the adsorption equilibrium pressures were set to 1 MPa and 1.5 MPa. The schematic diagram of the experimental equipment is shown in Figure 1. Methane (CH_4) was selected as the gas in the adsorption and desorption experiments. Vibration was applied after the coal reached adsorption equilibrium to allow desorption for 60 min. Previous research [13,14] showed that the natural frequency of coal was within 50 Hz, the mechanical vibration frequency that may induce coal and gas outburst accidents caused by underground operation was 5~100 Hz [17,18], and the vibration frequency of micro-seismic was 0~35 Hz [33]. Therefore, combining the frequency of various vibration forms and the purpose of this study, the vibration frequency in this experiment was set to 0, 25, and 50 Hz. Following the desorption experiment, the coal samples were degasified and subjected to high-pressure mercury intrusion and low-pressure liquid nitrogen adsorption experiments to determine the pore structure.

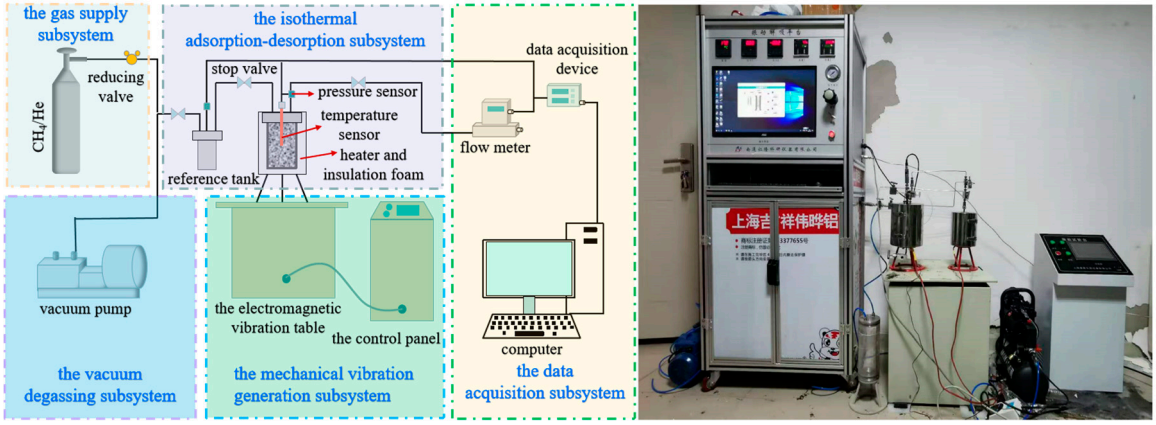


Figure 1. The schematic diagram and physical diagram of the MVGAD-I type vibration condition isothermal adsorption-desorption platform.

2.3. Multifractal Theory

The monofractal method describes or characterizes the porosity characteristics of the porous medium as a whole or as an average, thus only capable of describing the overall irregularity and heterogeneity within finite dimensions [34–37]. Unlike the monofractal method, the multifractal method can be decomposed into a series of interwoven fractal subsets that characterize the local variability and heterogeneity of the studied variables through a series of scaling indices, thus providing more accurate pore structure information [38–42]. These scaling indices can be calculated by using the pore structure test data obtained by the high pressure mercury intrusion experiment and the low pressure liquid nitrogen adsorption experiment according to Formulas (1)–(13).

The multifractal analysis on porous media with an interval of I = [a, b] necessitates the equal division of the interval into a set of boxes with a length of ε [40,41]. The dichotomy method is commonly used to divide the interval I = [a, b] with a length of L into $N(\varepsilon) = 2^k$ boxes with a length of $\varepsilon = L \cdot 2^{-k} (k = 0, 1, 2, 3, \cdots)$. Among these boxes, the mass probability function of the *i*-th box with a length of ε can be expressed as follows [39,42,43]:

$$P_i(\varepsilon) = \frac{N_i(\varepsilon)}{N_t} \tag{1}$$

where $N_i(\varepsilon)$ is the total number of study subjects in the *i*-th box, and N_t is the total number of study subjects in all boxes throughout the interval.

The partition function associated with q and $\chi(q, \varepsilon)$ (also known as the statistical moment function) is an important intermediate variable in multifractal calculations and can be derived from the following equation [44]:

$$\chi(q, \varepsilon) = \sum_{i=1}^{N(\varepsilon)} P_i^q(\varepsilon) \sim \varepsilon^{\tau(q)} \tag{2}$$

where q is the statistical moment order, a real number generally within [–10, 10], and $\tau(q)$ is the mass scaling function of q.

The mass scaling function $\tau(q)$ can also be expressed as follows:

$$\tau(q) = \lim \left[\ln \sum_{i=1}^{N(\varepsilon)} P_i^q(\varepsilon) / \ln(1/\varepsilon) \right] \tag{3}$$

Then, the generalized fractal dimension spectrum $D(q)$ can be determined as follows:

$$D_q = \frac{1}{q-1} \lim \frac{\log \chi(q, \varepsilon)}{\log \varepsilon} = \frac{\tau(q)}{q-1} (q \neq 1) \tag{4}$$

With q = 0, 1, and 2, D_0, D_1 and D_2 are defined as the capacity dimension, information dimension, and correlation dimension, respectively [43].

With q = 1, D_1 can be solved by L'Hospital's rule to make the D_q function continuous, as follows [45]:

$$D_1 = \lim_{\varepsilon \to 0} \frac{\sum_{i=1}^{N(\varepsilon)} P_i(1,\varepsilon) \log[P_i(1,\varepsilon)]}{\log(\varepsilon)} \tag{5}$$

If ε is small enough, then, $P_i(\varepsilon)$ is almost evenly distributed within each sub-interval, and $P_i(\varepsilon)$ and ε have the following relationship:

$$P_i(\varepsilon) \propto \varepsilon^{\alpha} \tag{6}$$

where α is the singularity exponent, reflecting the local singularity strength of the mass probability function $P_i(\varepsilon)$.

Different sub-intervals may have different α values, and the singularity exponent α can be calculated as follows [46]:

$$\alpha(q) \propto \frac{\sum_{i=1}^{N(\varepsilon)} [u_i(q,\varepsilon) \cdot \log \varepsilon]}{\log \varepsilon} \tag{7}$$

Among them, $u_i(q,\varepsilon)$ can be calculated as follows:

$$u_i(q,\varepsilon) = \frac{P_i^q(\varepsilon)}{\sum_{i=1}^{N(\varepsilon)} P_i^q(\varepsilon)} \tag{8}$$

The number of boxes with the same α value, denoted as $N_\alpha(\varepsilon)$, changes exponentially with the scale ε, i.e.,

$$N_\alpha(\varepsilon) \sim \varepsilon^{-f(\alpha)} \tag{9}$$

where $f(\alpha)$ is the multifractal singularity spectrum, representing the fractal dimension with the same singularity exponent subset.

$f(\alpha)$ can be calculated as follows [47]:

$$f(\alpha) \propto \frac{\sum_{i=1}^{N(\varepsilon)} [u_i(q,\varepsilon) \log u_i(q,\varepsilon)]}{\log \varepsilon} \tag{10}$$

The mass scaling function $\tau(q)$ and the generalized fractal dimension D_q have the following relationship:

$$\tau(q) = (q-1)D_q \tag{11}$$

The B.B. Hotdot pore classification method [36] was adopted in this study. The mercury intrusion method was used to quantitatively characterize the macropores (100 < d < 10,000 nm) and mesopores (100 < d < 100 nm)above 100 nm, and the low-pressure nitrogen adsorption method was used to characterize the minipores (10 < d < 100 nm)and micropores (d < 10 nm) in the coal mass.

3. Results and Discussion

3.1. Vibration-Affected Tectonic Coal Pore Structure Characteristics

3.1.1. Pore Size Distribution and Volume Change Characteristics of Macropores and Mesopores in Vibration-Affected Tectonic Coal

Based on the high-pressure mercury intrusion data, the pore size distribution and pore volume change characteristics of the tectonic coal before and after vibration at different frequencies are obtained, as shown in Figure 2. As shown in Figure 2, the macropore and mesopore volumes of the WXZ and GH coal samples increase with increasing vibration frequencies. After the WXZ coal sample was subjected to 25 Hz and 50 Hz vibration, the macropores were enlarged by 11.45% and 28.84%, respectively, compared with the coal

samples without vibration, and the mesopore volume was increased by 10.06% and 28.72%, respectively. After the GH coal sample was subjected to 25 Hz and 50 Hz vibration, the macropores were 1.66 times and 3.27 times those of the coal sample without vibration, respectively, and the mesopore volume was increased by 1.46 times and 2.38 times, respectively. After the WXZ coal sample was subjected to 25 Hz and 50 Hz vibration, the total volume of macropores and mesopores increased by 12.32% and 28.74%, respectively. After the GH coal sample was subjected to 25 Hz and 50 Hz vibration, the total volume of macropores and mesopores increased by 1.09 times and 2.79 times, respectively. Thus, low-frequency mechanical vibration can increase the volume of macropores and mesopores in tectonic coal, and the effect gradually increases with the increase in vibration frequency.

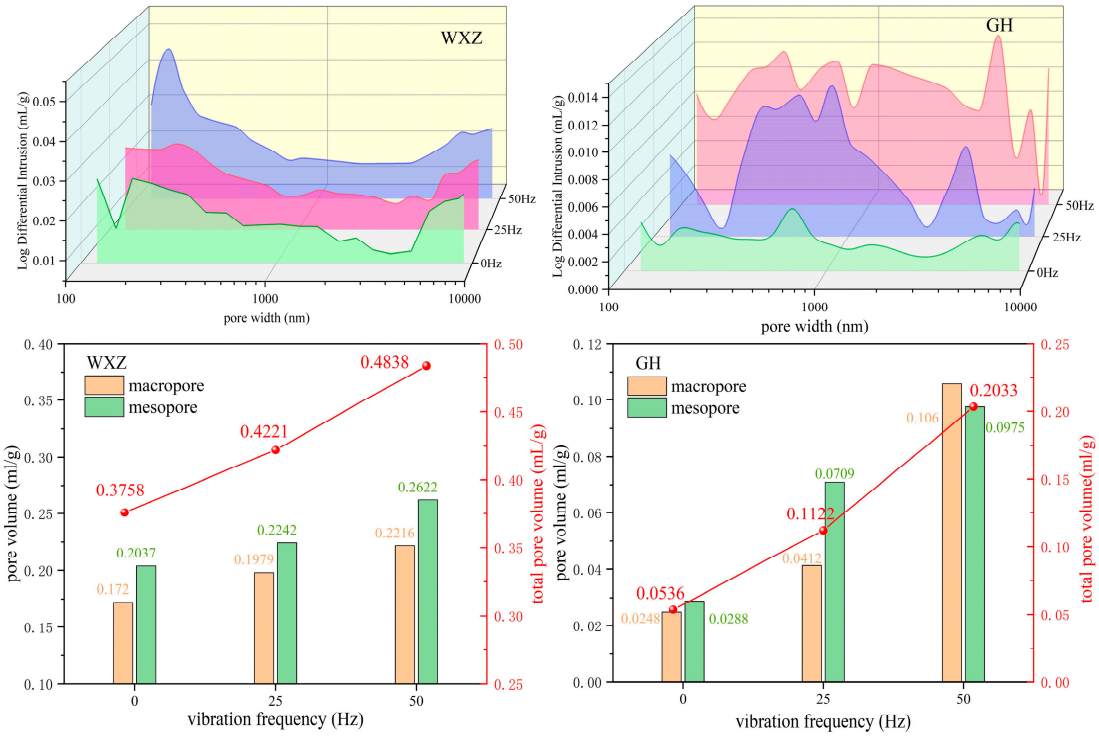


Figure 2. Size distribution and volume change characteristics of macropores and mesopores in vibration-affected tectonic coal.

According to the pore size distribution of the coal sample in Figure 2, the vibration increases in the volume of the mesopores with diameters of 100 to 200 nm and macropores with diameters of 3000 to 5000 nm in the WXZ coal sample. Among them, the 50 Hz vibration significantly increases the volume of mesopores, which range from 100 to 200 nm in size. The volume of pores with diameters of 300 to 5000 nm in the GH coal sample increased significantly after vibration. With decreased pore size, the macropore and mesopore size distributions of the coal sample change significantly after vibration, showing a unimodal and multimodal distribution. These results further indicate that vibration significantly affects the size distribution of macropores and mesopores, and the effect is stronger under greater frequencies.

3.1.2. Size Distribution and Volume Change Characteristics of Minipores and Micropores in Vibration-Affected Tectonic Coal

Figure 3 shows the size distribution and volume change characteristics of minipores and micropores in vibration-affected tectonic coal. As shown in Figure 3, the size distribution of minipores and micropores in the WXZ and GH coal samples is clearly multimodal. The pore size distribution of the WXZ coal sample increases with the increase in pore size, while that of the GH coal sample is uniformly distributed with the increase in pore size.

The vibration significantly increased the volume of minipores 40 to 100 nm in size in the GH coal sample, and the pore volume significantly increased in the coal sample after 50 Hz vibration. The effect of vibration on the size distribution of minipores and micropores in the WXZ coal sample is not obvious.

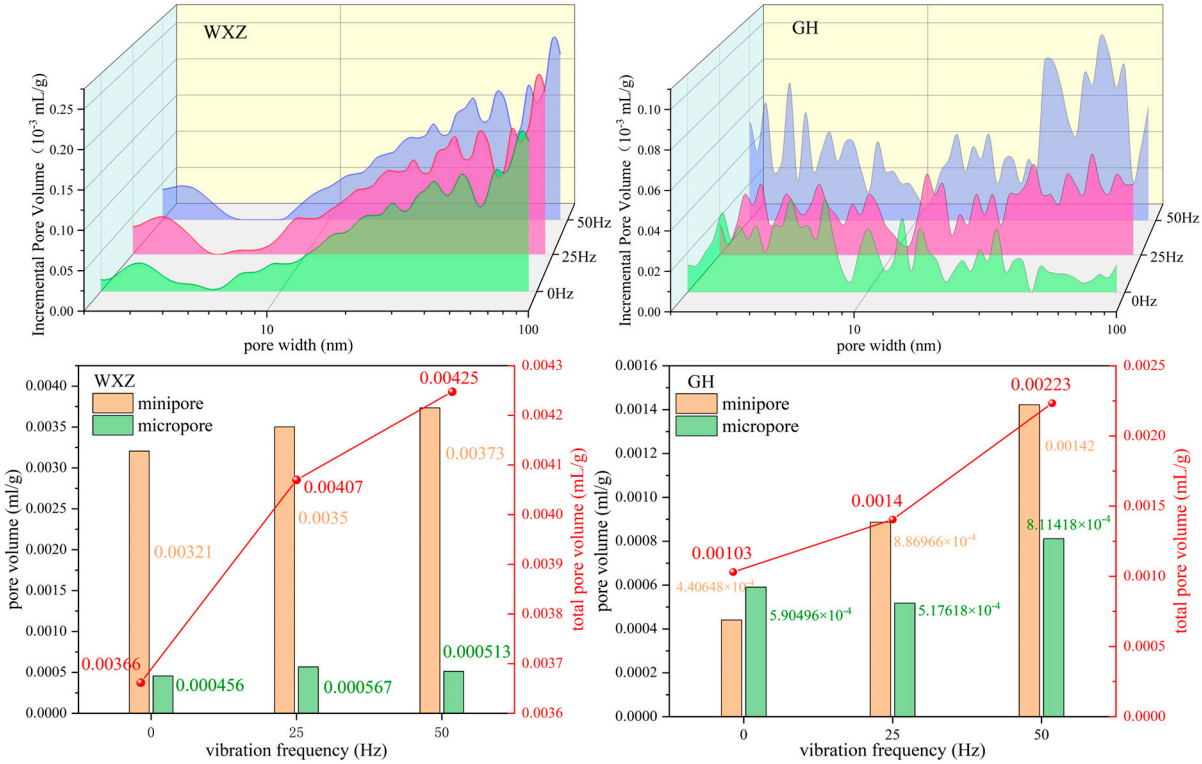


Figure 3. Pore size distribution and volume change characteristics of minipores and micropores in vibration-affected tectonic coal.

The 25 Hz and 50 Hz vibrations caused the minipore volume of the WXZ coal sample to increase by 9.03% and 16.19%, respectively, and the micropore volume by 24.34% and 12.50%, respectively. After the 25 Hz and 50 Hz vibrations, the minipores in the GH coal sample become 2.01 times and 3.22 times that in the coal sample without vibration. The 25 Hz vibration reduced the micropore volume of the GH coal sample by 12.34% but increased the micropore volume by 37.41%. After the WXZ coal sample was subjected to 25 Hz and 50 Hz vibration, the total volume of minipores and micropores increased by 11.20% and 16.12%, respectively. After the GH coal sample was subjected to 25 Hz and 50 Hz vibration, the total volume of macropores and mesopores increased by 35.92% and 116.50%, respectively. The vibration has a greater impact on the distribution and pore volume of minipores and micropores in the GH coal sample than in the WXZ coal sample. Overall, the effect of vibration on the minipores and micropores in tectonic coal increases with the increase in frequency.

3.2. Multifractal Characteristics of the Pore Structure of the Vibration-Affected Tectonic Coal

The pore interval for the multifractal calculation of macropores and mesopores was I = [100, 10,000 nm], the pore interval for the multifractal calculation of minipores and micropores was I = [1, 100 nm], and the statistical moment order q was set to all integers in [−10, 10]. Previous studies have confirmed that the research subjects have multifractal characteristics if there is a linear relationship between $\log(\varepsilon)$ and $\log \chi(q, \varepsilon)$. Figure 4 reflects the characteristics of the fitting between the partition function $\chi(q, \varepsilon)$ of the size distribution of macropores and mesopores in vibration-affected tectonic coal and the sub-interval length ε. Figure 5 reflects the characteristics of the fitting between the partition function $\chi(q, \varepsilon)$ of

the size distribution of minipores and micropores in vibration-affected tectonic coal and the sub-interval length ε. The fitting results showed a significant linear relationship between the $\log(\varepsilon)$ of the pore size distributions of all WXZ coal samples and GH coal samples and $\log \chi(q, \varepsilon)$, indicating that the generalized fractal dimension can be used to characterize the multifractal characteristics of the pores in the coal samples.

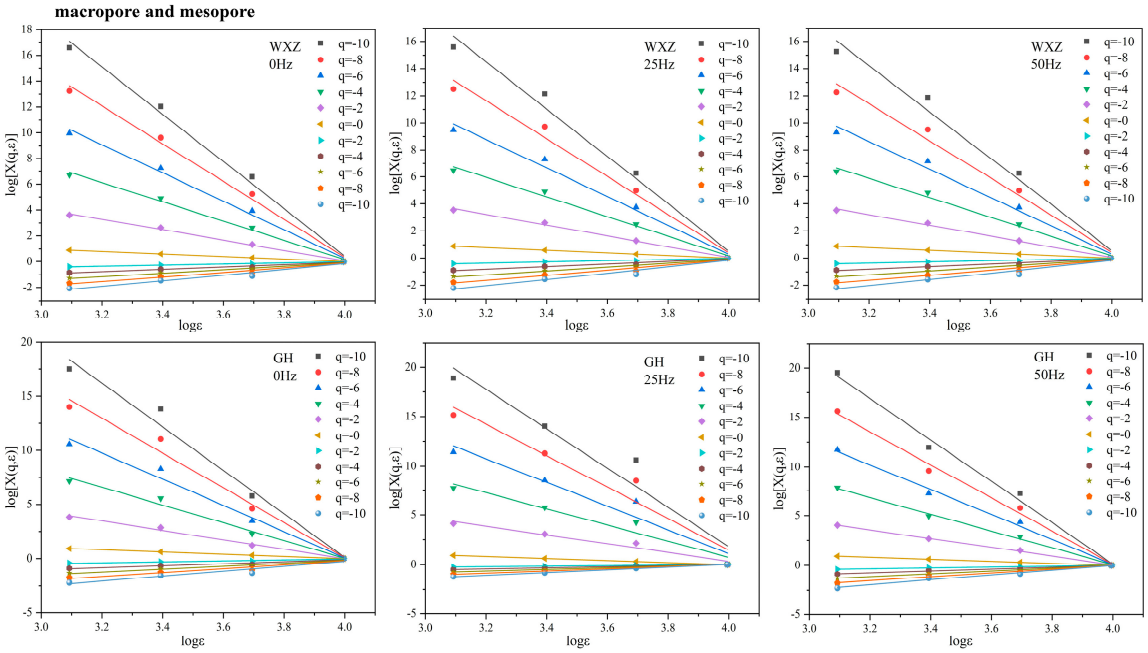


Figure 4. Fitting curves between the partition function of macropores and mesopores and the interval length of vibration-affected tectonic coal.

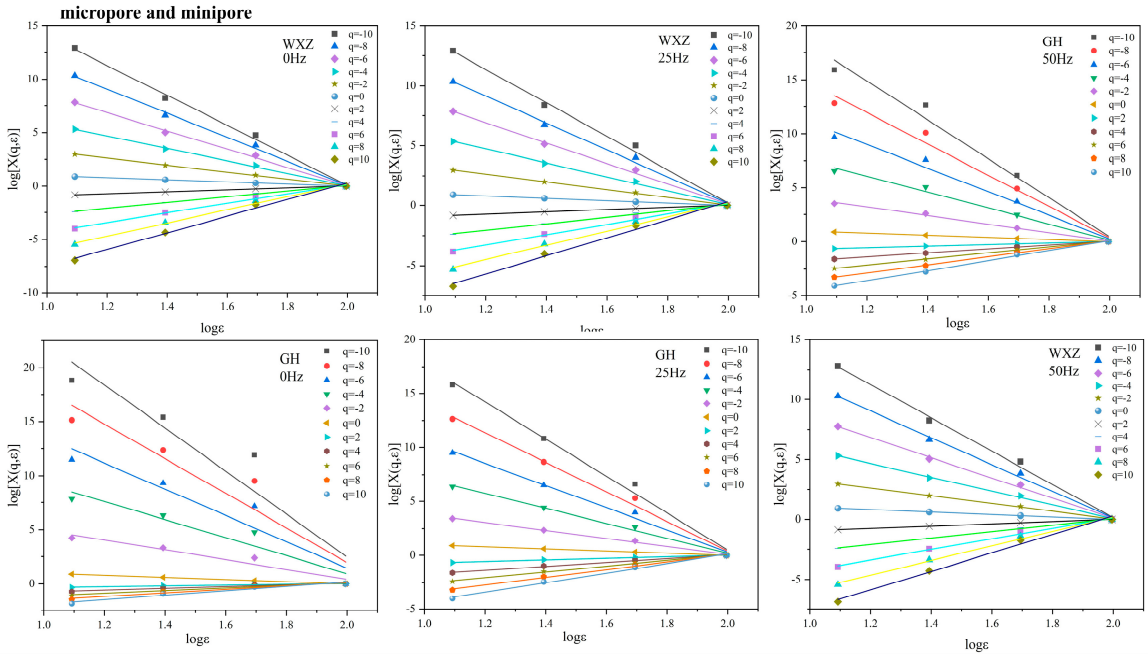


Figure 5. Fitting curves between the partition function of minipores and micropores and the interval length of vibration-affected tectonic coal.

As q gradually increased from −10 to 10, the fitting curve gradually shifted from negative correlation to positive correlation, with gradually increased density, indicating that the pore

size of the coal was unevenly distributed and clustered in the studied small range. This is consistent with the pore size distribution characteristics shown in Figures 2 and 3.

The generalized dimension spectrum D(q)~q of the pore size distribution of the vibration-affected tectonic coal is shown in Figure 6. The generalized dimension spectral curves of the pores of all tectonic coal samples show trends in an inverse "S" shape, with maximum and minimum values, indicating that the pore size distribution has non-uniform characteristics.

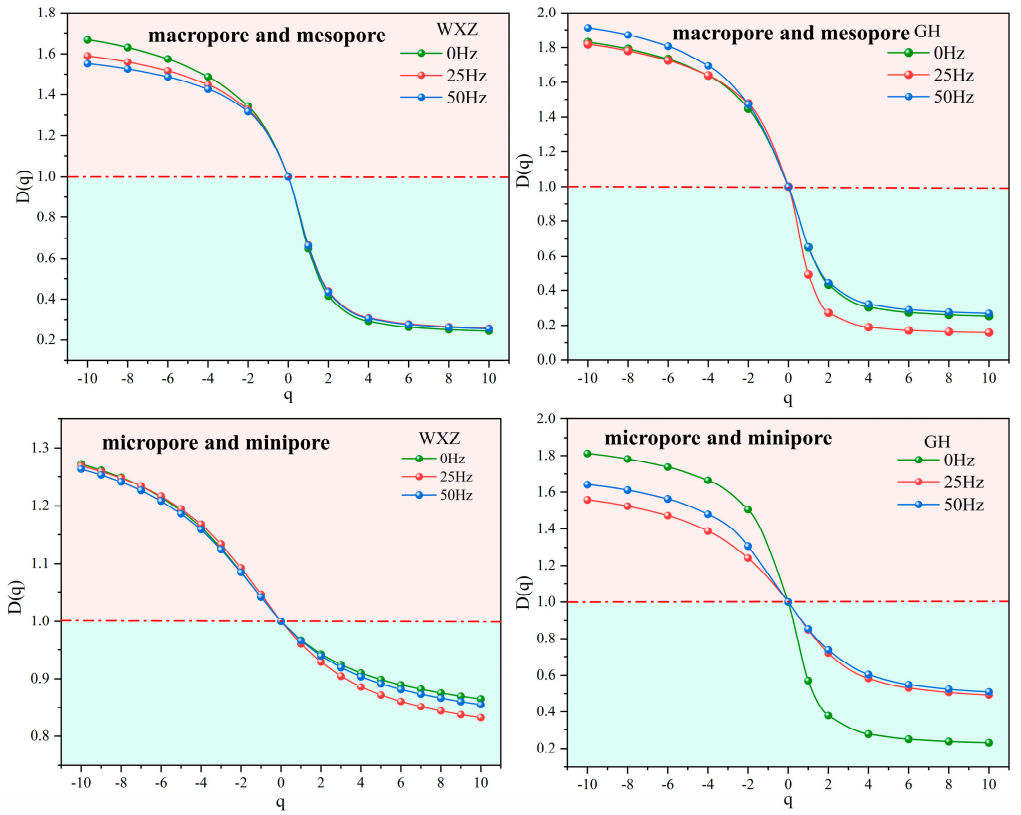


Figure 6. The generalized dimension spectra of the macropore and mesopore size distribution in the vibration-affected tectonic coal.

According to the generalized fractal dimension spectra, characteristic parameters such as capacity dimension D_0, information dimension D_2, correlation dimension D_2, and spectral width D_{-10}–D_{10} can be obtained. These parameters can reflect the heterogeneity information of the pore distribution in the coal, as shown in Table 2. The capacity dimension D_0 reflects the scaling characteristics of non-empty boxes containing certain pores under continuous segmentation. The data in Table 2 show that the capacity dimension of all coal sample pores is 1, indicating the presence of data in all boxes. The capacity dimensions of all coal samples are the same because the same pore size range was selected as the study interval.

The information dimension D_1 reflects the concentration degree of the pore distribution as the pore size interval changes. The correlation dimension D_2 reflects the uniformity of the pore size distribution measurement intervals. A smaller D_1 value indicates a more concentrated pore distribution, while a larger D_2 value indicates a more evenly spaced pore size distribution [27]. The D_1 value is selected for detailed analysis in this study. The D_1 values of the macropores and mesopores in the WXZ coal samples after vibration are greater than those of the coal samples without vibration, and the 25 Hz vibration causes the D_1 values of the minipores and micropores to fall below those of the coal samples without vibration. The D_1 values of the minipore and micropore distributions of the GH coal sample after vibration are greater than those of the coal sample without vibration.

The 25 Hz vibration significantly decreased the D_1 values of the macropore and mesopore distributions in the GH coal sample, indicating that the 25 Hz vibration increased the degree of local concentration of the macropore and mesopore distributions. The 50 Hz vibration slightly increased the D_1 values of the macropore and mesopore distributions in the GH coal sample. Thus, vibration changes the local concentration of pore distribution in tectonic coal. Overall, the 50 Hz vibration causes the pore distribution in coal to become more uniform.

Table 2. Characteristic parameters of the generalized fractal dimension spectra of the pore structure of the vibration-affected tectonic coal.

Coal Sample	Pore Type	Frequency (Hz)	D_0	D_1	D_2	D_{-10}–D_{10}
WXZ	macropore and mesopore	0	1	0.6488	0.4155	0.7567
		25	1	0.6668	0.4377	1.3321
		50	1	0.6639	0.4335	1.2978
	micropore and minipore	0	1	0.9656	0.9390	0.4076
		25	1	0.9600	0.9284	0.4369
		50	1	0.9669	0.94202	0.4086
GH	macropore and mesopore	0	1	0.6520	0.4322	1.5747
		25	1	0.4930	0.2733	1.6603
		50	1	0.6536	0.4454	1.6411
	micropore and minipore	0	1	0.5714	0.3783	1.5806
		25	1	0.8482	0.7192	1.0662
		50	1	0.8535	0.7374	1.1304

The spectral width D_{-10}–D_{10} reflects the discrepancy characteristics of the pore size distribution in the local interval, which can characterize the heterogeneity of the pore structure in the coal sample. A larger D_{-10}–D_{10} value indicates greater local fluctuations in the pore size distribution and a more complex pore structure [46]. The increased D_{-10}–D_{10} of macropores and mesopores in the WXZ coal samples and the GH coal samples after vibration indicates that the vibration increased the local fluctuations of the macropore and mesopore size distribution of the tectonic coal. After vibration, the D_{-10}–D_{10} of the minipores and micropores in the WXZ coal sample increased slightly, and the D_{-10}–D_{10} of the GH coal sample decreased. Thus, vibration can change the complexity of the minipore and micropore size distributions.

The multifractal singularity spectra of the pore size distribution in the coal samples are shown in Figure 7. In the coal samples after vibration at different frequencies, the multifractal singularity spectra of pore size distribution are characterized by an inverted U-shaped unimodal convex function, which is another typical feature of the study subjects consistent with multifractal distribution. According to the multifractal singularity spectrum curve, the multifractal singularity spectrum characteristic parameters can be calculated, as shown in Table 3. The pore size distribution mass scaling function $\tau(q)$ curve (Figure 8) of vibration-affected tectonic coal is an obvious two-stage convex function, once again proving the multifractal characteristics of the pore structure of vibration-affected tectonic coal.

The singularity exponent α_0, also known as the Hausdorff dimension, can reflect the degree of local concentration of the pore size distribution, and a larger value indicates a smaller degree of local concentration [44]. The singularity exponents α_0 of the macropores and mesopores in the WXZ and GH coal samples after vibration are greater than those of the coal samples without vibration, indicating that the vibration increased the local distribution fluctuations and local concentration degrees of the macropores and mesopores of the tectonic coal. Except for the GH coal sample subjected to 25 Hz vibration, the singularity exponent α_0 of the minipores and micropores of other coal samples with vibration is greater than that of the coal samples without vibration. Overall, the vibration reduces the local concentration of the pores in the tectonic coal, rendering their distribution more uniform.

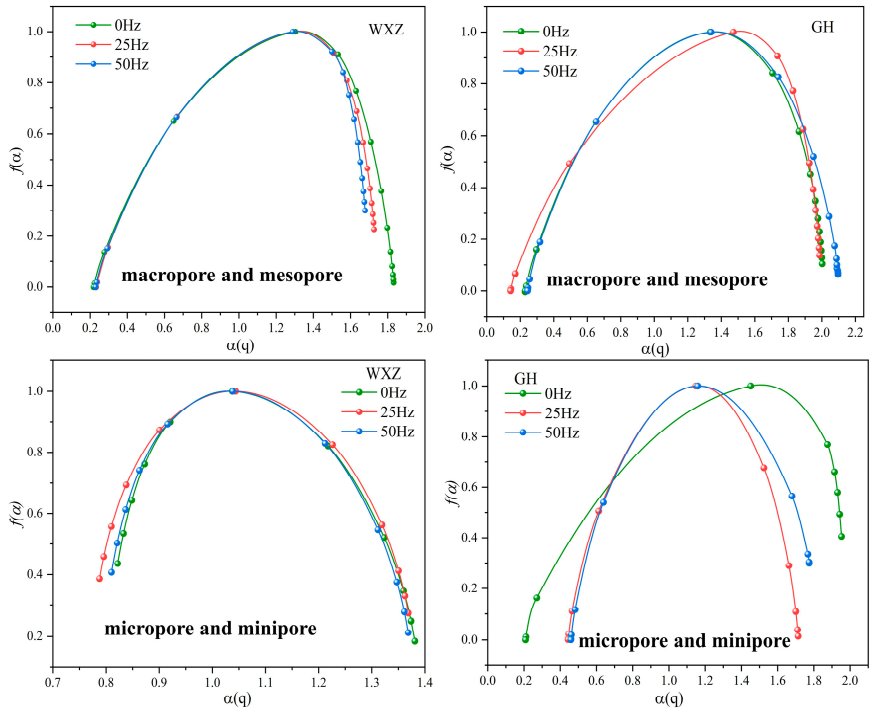


Figure 7. Generalized dimension spectra of the pore size distribution of vibration-affected tectonic coal.

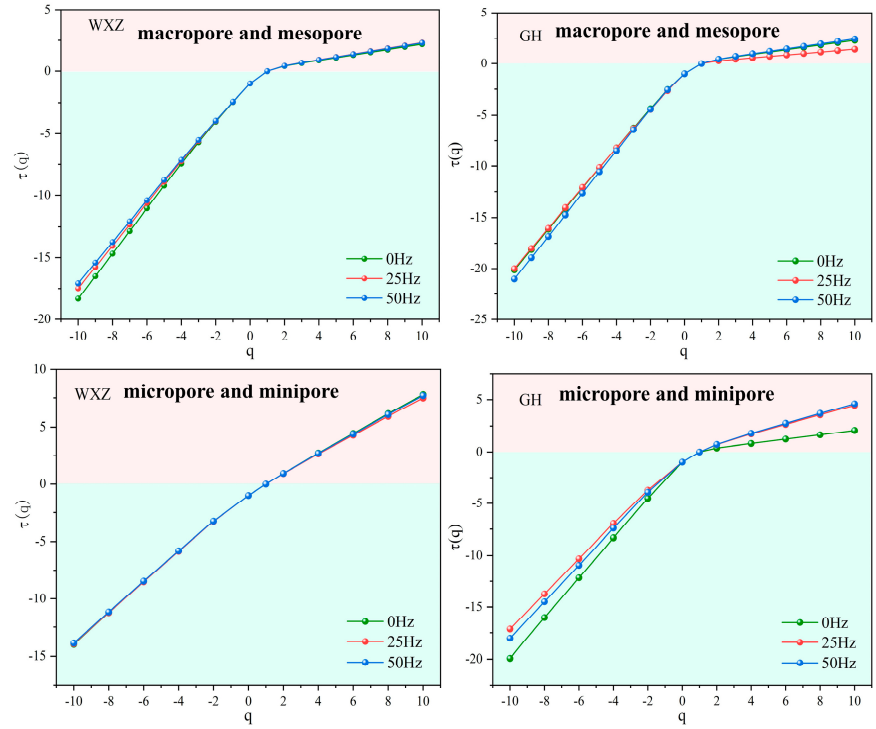


Figure 8. Mass scaling function $\tau(q)$ of pore size distribution of vibration-affected tectonic coal.

Table 3. Characteristic parameters of the generalized dimension spectrum of the pore size distribution of vibration-affected tectonic coal.

Coal Sample	Frequency (Hz)	Macropore and Mesopore			Micropore and Minipore		
		α_0	$\Delta\alpha$	Δf	α_0	$\Delta\alpha$	Δf
WXZ	0	1.2891	1.6127	0.0166	1.0375	0.5584	−0.2509
	25	1.3034	1.4943	0.2262	1.0438	0.5810	−0.1120
	50	1.2894	1.4485	0.3004	1.0383	0.5592	−0.1947
GH	0	1.3337	1.7727	0.1046	1.4511	1.7444	0.4051
	25	1.4722	1.8442	0.1374	1.1479	1.2698	0.0135
	50	1.3392	1.8531	0.0632	1.1591	1.3154	0.2983

The spectral width $\Delta\alpha$ ($\alpha_{max} - \alpha_{min}$) of the multifractal singularity spectrum can characterize the complexity of the probabilistic measure distribution of the entire pore size space, and a larger value indicates more significant differences within the multifractal measurement system and a more uneven distribution [40]. The vibration reduced the $\Delta\alpha$ of macropores and mesopores in the WXZ coal samples, and that of the minipores and micropores in the GH coal samples showed the opposite trend. The changes in the spectral width $\Delta\alpha$ of the pores in the GH coal samples after vibration are opposite to those of the WXZ coal samples. These results show that vibration can change the uniformity of the pore distribution in tectonic coal, altering the degree of difference in the pore size distribution. Since coal is a complex porous medium, a single parameter cannot effectively reflect the changes in its pore structure. Therefore, it is necessary to continue to analyze another characteristic parameter Δf of the multifractal singular spectrum and the parameter characterizing pore connectivity.

$\Delta f(f(\alpha_{max}) - f(\alpha_{min}))$ characterizes the ratio of the maximum and minimum number of elements in the subset of relevant physical parameters [41]. When the small probability subset predominates, the multifractal singularity spectrum shows a right-hook shape, that is, $\Delta f > 0$. The Δf of the macropore and mesopore distributions in the WXZ and GH coal samples showed obvious right hook shapes, and the difference was not obvious. Thus, the macropores and mesopores in the vibration-affected tectonic coal have small-range aggregation characteristics, and this characteristic plays a dominant role in the heterogeneity of the pore size distribution, but the vibration does not cause significant changes in its heterogeneity. The Δf of the minipore and micropore distributions in the GH coal sample were above 0, but the obvious right hook-shaped trend gradually weakened after vibration. The Δf of the minipore and micropore distributions in the WXZ coal sample were below 0, but the changes before and after vibration are not obvious. These results show that vibration can change the heterogeneity and aggregation characteristics of pore distribution in tectonic coal, but the effect is not significant.

The Hurst index can be used to characterize pore connectivity and can be derived using the multifractal mass scaling function $\tau(q)$ and the multifractal singularity spectrum $f(\alpha)$. The calculation is as follows [42,46]:

$$H(q) = \frac{\tau(q) + 1}{q} \tag{12}$$

$$\tau(\alpha) = q\alpha(q) - f(\alpha) \tag{13}$$

where *H(q)* is the Hurst index, which characterizes the pore connectivity.

With q = 2, the classical Hurst index can be calculated using the above two equations, and a smaller value indicates poorer pore connectivity in the medium [39,44]. The Hurst indices of the pores of all grades in the tectonic coal after vibration at different frequencies are presented in Figure 9. The Hurst indices of macropores, mesopores, minipores, and micropores in all WXZ coal samples and GH coal samples after vibration were greater than those of the coal samples without vibration, showing increasing trends with the

increase in vibration frequency. Thus, vibration increases the pore connectivity in the coal. Studies have shown that pore connectivity affects coal permeability, and the permeability is higher with better pore connectivity. Therefore, vibration can increase the permeability of tectonic coal.

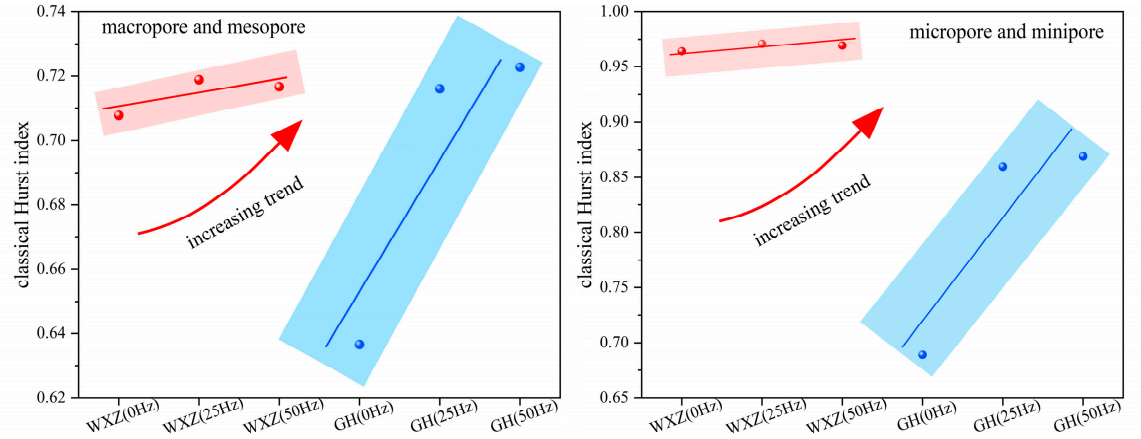


Figure 9. Classic Hurst index of vibration-affected tectonic coal pores.

3.3. Characteristics of Gas Desorption in Vibration-Affected Tectonic Coal

The gas desorption characteristics of tectonic coal samples with different adsorption equilibrium pressures at different vibration frequencies are shown in Figure 10. When the equilibrium pressure is 1 MPa, the desorption of the WXZ coal sample under 25 Hz and 50 Hz vibration increases by 7.02% and 13.38% compared with 0 Hz, respectively. The desorption of GH coal samples subjected to vibration at 25 Hz and 50 Hz increases by 18.83% and 32.31% compared with 0 Hz, respectively. At an equilibrium pressure of 1.5 MPa, the desorption of the WXZ coal sample under 25 Hz and 50 Hz vibration increases by 9.70% and 16.67% compared with 0 Hz, respectively. The desorption of GH coal samples subjected to vibration at 25 Hz and 50 Hz increases by 26.21% and 39.51% compared with 0 Hz, respectively. At the same vibration frequency, the cumulative gas desorption of the same coal sample at the same moment increases with increasing adsorption equilibrium pressure. A higher adsorption equilibrium pressure and a concentration difference drive the rapid desorption and diffusion of the gas, resulting in more gas being desorbed in the same period. The gas desorption amount of all coal samples subjected to vibration is greater than that of coal samples without vibration, indicating that mechanical vibration can promote gas desorption in tectonic coal.

The adsorption equilibrium pressure of gas in coal determines the size of its internal gas concentration, with a higher pressure resulting in a higher concentration of desorbed gas inside the coal pore fissures during the desorption process. Consequently, the gas diffusion process becomes stronger, and the gas desorption rate is higher. Figure 11 shows the initial gas desorption rate of tectonic coal samples subjected to vibration at different adsorption equilibrium pressures. It can be seen that a larger adsorption equilibrium pressure leads to a higher initial gas desorption rate when the coal sample is subjected to the same frequency vibration. However, the initial gas desorption rate of vibration-affected coal samples is greater than that of unaffected coal samples, regardless of the adsorption equilibrium pressure, with a larger frequency resulting in a higher value. These results indicate that vibration improves the initial gas desorption capacity of tectonic coals.

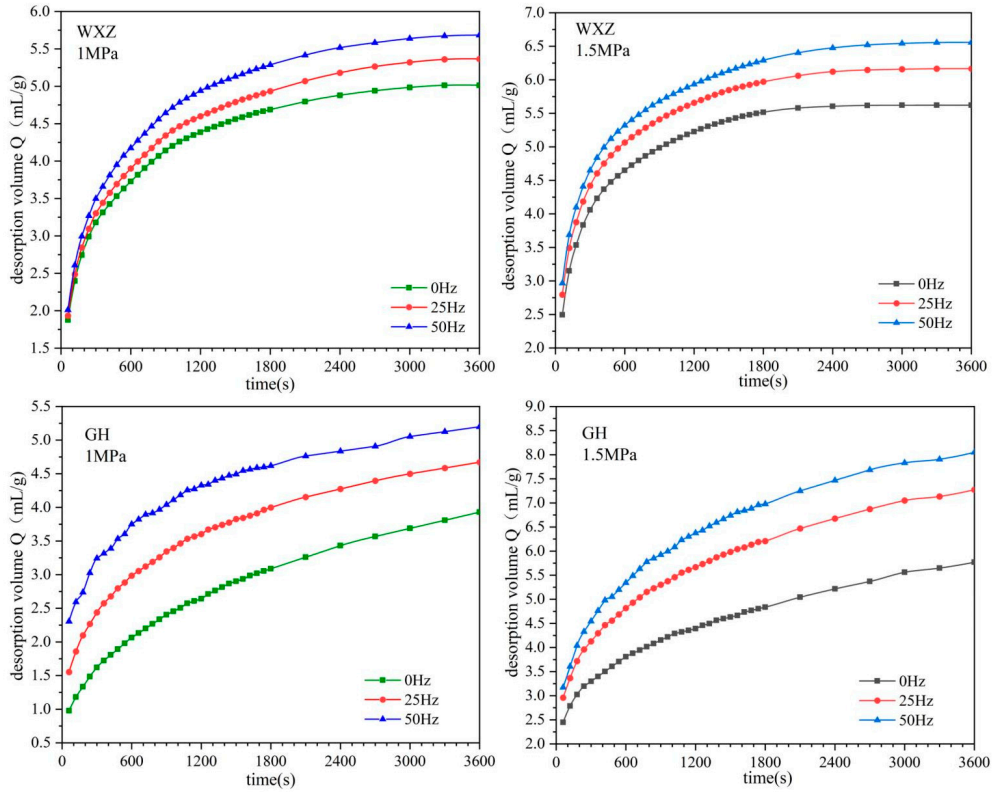


Figure 10. Gas desorption curves of coal samples.

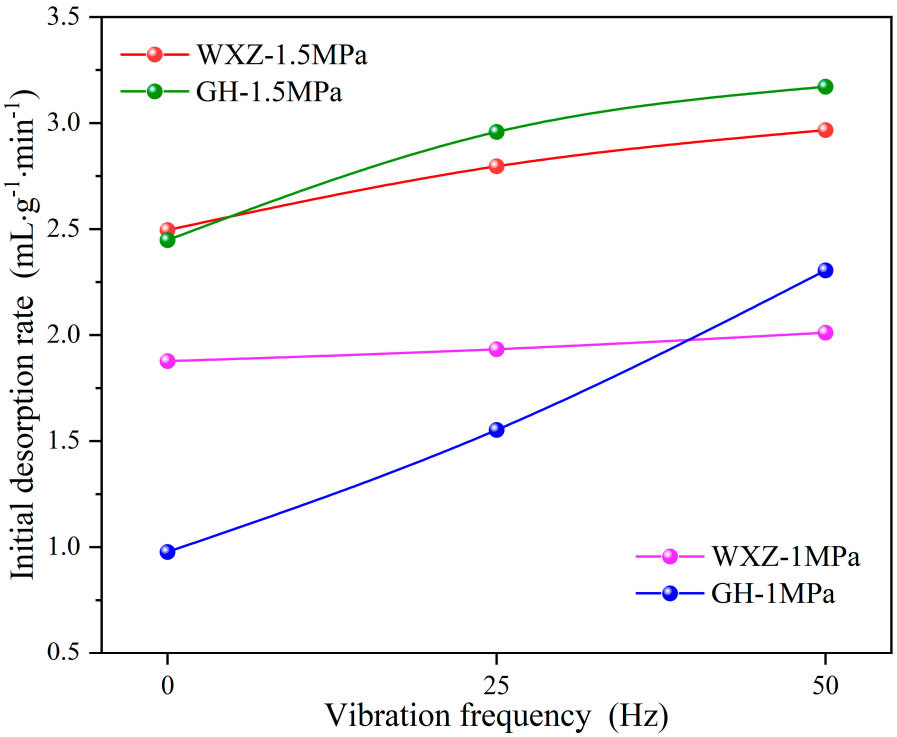


Figure 11. Initial gas desorption rate of vibration-affected tectonic coal.

3.4. Characteristics of Gas Diffusion in Vibration-Affected Tectonic Coals

The transport of gas (the main component is methane CH_4) from coal to the external environment involves a desorption-diffusion-seepage process [28,29,48,49]. For granular coal, scholars generally agree that the diffusion of gas from the coal matrix pores to the

particle surface needs to undergo rapid gas desorption on the pore surface and diffusion in the matrix pore fracture system. Li et al. [50] proposed a kinetic diffusion coefficient model for gas diffusion in multiscale, multilevel pores of coal particles based on the classical single-pore model for unsteady diffusion in homogeneous granular coal. The analytical solution of the dynamic diffusion coefficient model is as follows [18,48–50]:

$$\frac{Q_t}{Q_\infty} = 1 - \frac{6}{\pi^2}\sum_{n=1}^{\infty}\frac{1}{n^2}\exp\left(-\frac{n^2\pi^2 D_0}{r0_2\beta}(1-e^{-\beta t})\right) \tag{14}$$

$$D(t) = D_0\exp(-\beta t) \tag{15}$$

where Q_t is the total amount of gas desorption from coal particles at time t, mL/g, and r_0 is the radius of coal particles, cm. The average value of the corresponding particle size is taken. Q_∞ is the maximum gas desorption amount, mL/g; $D(t)$ is the kinetic diffusion coefficient, cm^2/s; D_0 is the initial gas diffusion coefficient at time t = 0, cm^2/s; and β is the diffusion coefficient attenuation coefficient, s^{-1}.

The initial effective gas diffusion coefficient D_e can better reflect the gas diffusion capacity at the initial stage of desorption, and its expression is as follows:

$$D_e = \frac{D_0}{r_0^2} \tag{16}$$

Q_∞ can be calculated using the following equation:

$$Q_\infty = \left(\frac{abP}{1+bP} - \frac{abP_0}{1+bP_0}\right)\left(1 - W_f - A_f\right) \tag{17}$$

where a is the gas adsorption constant, indicating the maximum adsorption amount of coal under the experimental conditions, mL/g; b is the gas adsorption constant, MPa^{-1}; W_f is the moisture of coal, %; A_f is the ash of coal, %; and P and P_0 are the adsorption equilibrium pressure and atmospheric pressure, respectively, MPa, which, at this time, is P_0= 0.1 MPa.

The fitting effect between the measured gas diffusion of the coal sample and the dynamic diffusivity model is shown in Figure 12. The fitted correlation coefficients for WXZ coal samples at equilibrium pressures of 1 MPa and 1.5 MPa are 0.9993 to 0.9997 and 0.9556 to 0.9902, respectively. The fitted correlation coefficients for GH coal samples at equilibrium pressures of 1 MPa and 1.5 MPa are 0.9442 to 0.9929 and 0.8999 to 0.9593, respectively. The above results show that the dynamic diffusion coefficient model is applicable to the gas diffusion characteristics of vibration-affected tectonic coal.

The kinetic parameters of gas diffusion in vibration-affected tectonic coal D_0, D_e, and β were obtained by fitting the kinetic diffusion coefficient model, as shown in Table 4. Figure 13 reflects the trend of the initial gas effective diffusion coefficient of the vibration-affected tectonic coal. Both the initial gas diffusion coefficient and the initial gas effective diffusion coefficient of coal samples with different equilibrium pressures at the same frequency exhibit an increasing trend, as evidenced by Table 4 and Figure 13. This trend arises from the positive correlation between adsorption equilibrium pressure and gas adsorption in coal, resulting in an increased gas concentration. The diffusion process in the early desorption stage mainly occurs in pores with large pore sizes, and its diffusion resistance is relatively small. Subsequently, a higher adsorption equilibrium pressure leads to a greater concentration difference between inside and outside the coal particles. Consequently, the diffusion drive becomes greater, resulting in a greater initial effective gas diffusion coefficient.

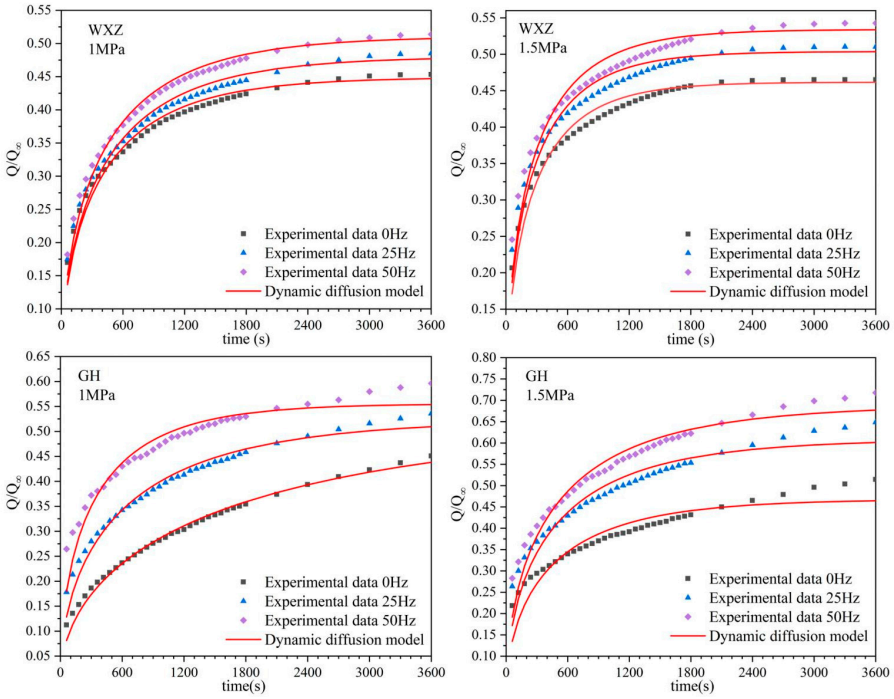


Figure 12. Measured gas diffusion rate of coal samples fitted with the kinetic diffusion model.

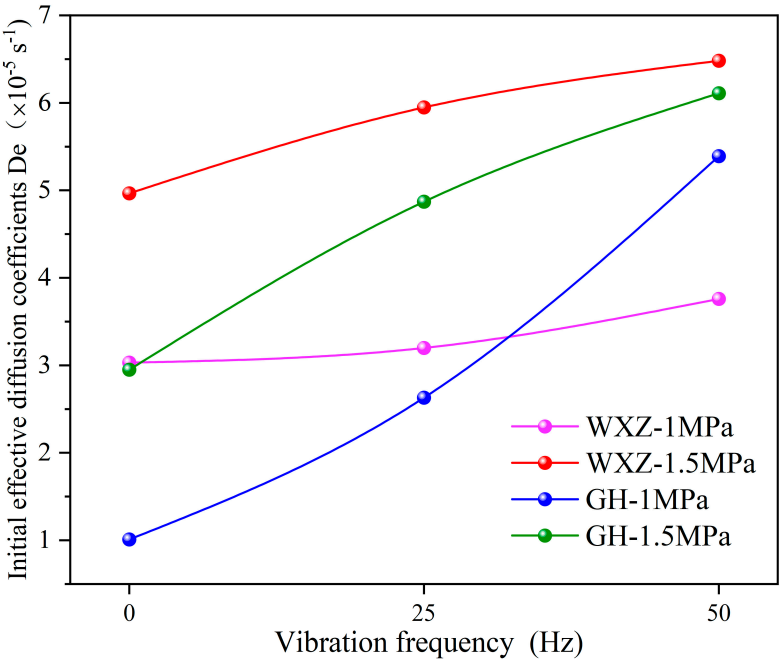


Figure 13. Initial effective diffusion coefficient of vibration-affected tectonic coal.

The attenuation coefficients of gas diffusion in coal samples do not show a uniform trend with increasing vibration frequency, owing to the intricate dynamics involved in the process of gas diffusion. Variations in pore connectivity, tortuosity of pore channels, complexity of pore structure, and pore sizes collectively contribute to disparities in resistance encountered during gas diffusion within coal. The energy required for diffusion, the length of the diffusion path, and the effective diffusion area also affect the diffusion capacity of the gas. The decay of diffusion capacity during diffusion is a multifactorial, coupled process.

Table 4. Kinetic parameters of gas diffusion in vibration-affected tectonic coals.

Coal Sample	Frequency (Hz)	1 MPa			1.5 MPa		
		D_0	D_e	β	D_0	D_e	β
WXZ	0	10.8	3.03	12.9	17.7	4.97	19.7
	25	11.4	3.19	11.6	21.2	5.95	19.1
	50	13.4	3.76	11.7	23.1	6.48	18.0
GH	0	4.04	1.01	3.01	11.8	2.95	11.3
	25	10.5	2.63	7.72	19.5	4.87	9.69
	50	21.6	5.39	13.6	24.4	6.11	8.65

Notes: $D_0(\times 10^{-7}\mathrm{cm}^2/\mathrm{s})$; $D_e(\times 10^{-5}/\mathrm{s})$; $\beta(\times 10^{-4}\mathrm{s}^{-1})$.

At the same equilibrium pressure, the initial gas diffusion coefficient and initial effective gas diffusion coefficient of the same coal under vibration are greater than those of the coal sample under non-vibration conditions. It indicates that vibration enhances the initial gas diffusion ability in tectonic coal, and the overall diffusion ability is stronger with higher frequency. The diffusion of gas (CH_4) molecules is affected by a series of physical effects of mechanical vibrations on the gas molecules and by the energy transfer resulting from this process. In addition, the increase in pore parameters, such as macroporous volume in granular coal due to mechanical vibration, facilitates the diffusion of initially desorbed gas.

3.5. Analysis of the Correlation between Multifractal Characteristics of Pore Space and Gas Desorption Capacity in Vibration-Affected Tectonic Coals

The pore volume, the degree of pore connectivity, the homogeneity of pore distribution, and the tortuosity of pore channels all determine the ease of gas diffusion and transport from coal particles to the outside environment. These pore characteristics determine the magnitude of parameters characterizing the gas desorption and diffusion capacity, such as the gas desorption volume Q, the initial desorption velocity V_0, the initial gas diffusion coefficient D_0, the initial effective diffusion coefficient D_e, and the diffusion attenuation coefficient β. Therefore, this paper conducts Pearson correlation analysis between the pore volume, multifractal characteristic parameters, and desorption parameters at various levels. The results are shown in Figure 14.

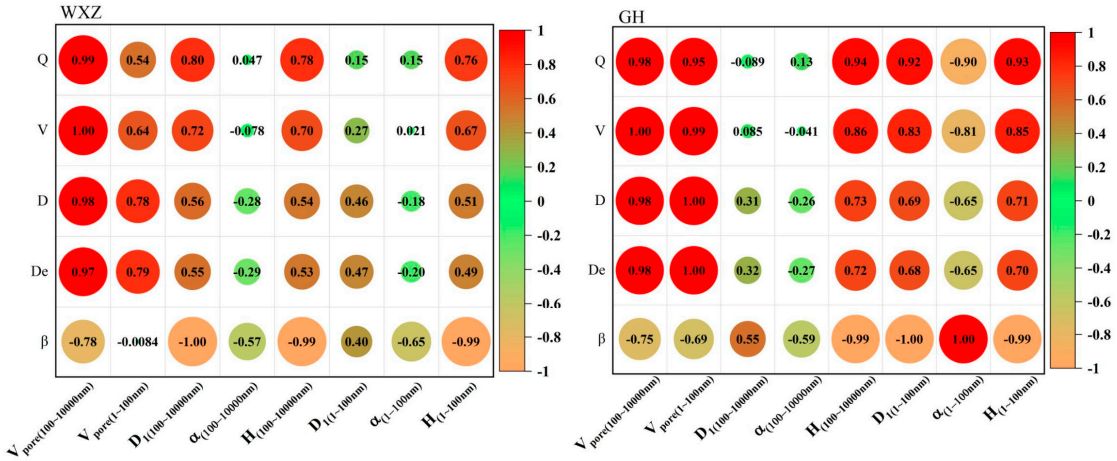


Figure 14. Correlation matrix between pore structure parameters and desorption-diffusion parameters.

It can be seen that Q, V_0, D_0, and D_e of the WXZ and GH coal samples have significant positive correlations with pore volume and Hurst index at all levels. It indicates that with a larger pore volume and pore connectivity, the initial gas desorption and diffusion capacity in coal is stronger. Q, V_0, D_0, and D_e of WXZ and GH coal samples have positive

correlations with the information dimension D_1 of all levels of pores, but Q, V_0, D_0, and D_e of GH coal samples show less significant correlations with D_1 of their large and medium pores. These results indicate that a larger D_1 leads to a more uniform pore distribution, which is conducive to the desorption and diffusion of gas. In contrast, V_0, D_0, and D_e of WXZ and GH coal samples and the Hausdorff dimension of all levels of pores α_0 have a negative correlation, but the differences are not significant. With a greater local concentration of pores in coal, the initial gas desorption and diffusion abilities of gas are weaker. Therefore, the multifractal parameters can reflect the compactness degree and uniformity of the pore distribution in coal, which affects the ability of gas desorption and diffusion. Finally, the β of the coal samples exhibits a negative correlation with the volume of pores at all levels, the Hausdorff dimension, and the Hurst index. This correlation suggests that a higher pore volume in tectonic coals results in a more even distribution of pores and greater connectivity among them, leading to a lower diffusion attenuation coefficient and enhanced gas (CH_4) diffusion ability.

According to the research results in Section 3.2, vibration increases the volume of pores in tectonic coal to a certain extent and reduces the density of the pore distribution in the coal. Consequently, the pore distribution in the coal is more uniform, with reduced complexity and increased connectivity of pores at all levels. This further proves that vibration can facilitate the gas desorption and diffusion abilities of tectonic coal.

4. Conclusions

(1) The results of high-pressure mercury intrusion and low-temperature liquid nitrogen adsorption experiments show that vibration affects the pore size distribution and pore volume characteristics of tectonic coals. Vibration causes an increase in pore volume in coal, and the expansion effect becomes stronger as the vibration frequency increases within the frequency range of 0–50 Hz. The increase in pore volume in coal provides more space for gas storage and transportation, and vibration is conducive to gas migration in coal.

(2) The pore structure of the vibration-affected tectonic coal has multiple fractal characteristics, and the pore size distribution has a small range clustering feature. Vibration changes the degree of concentration, heterogeneity, local fluctuations, complexity, and connectivity of the pore distribution in coal. The change in the multifractal characteristic parameters of the pore structure indicates that vibration reduces the local concentration of pore distribution in coal. As a result, the pore size distribution is more uniform, and the connectivity of pores increases at all levels, promoting gas desorption and diffusion in coal.

(3) The diffusion coefficient model is applicable to the gas diffusion characteristics of seismic coal structures. Vibration increases the gas desorption amount, initial desorption velocity, initial gas diffusion coefficient, and initial effective gas diffusion coefficient in tectonic coal. In addition, the desorption and diffusion ability of gas in structural coal is increased with vibration, and this ability becomes stronger as the vibration frequency increases within the frequency range of 0–50 Hz.

(4) Multifractal parameters can affect gas desorption and diffusion ability by reflecting the density, uniformity, and connectivity of pore distribution in coal. Gas desorption volume, initial desorption velocity, initial gas diffusion coefficient, and initial gas effective diffusion coefficient have a significant positive correlation with pore volume and Hurst index. In contrast, the initial gas desorption velocity, initial gas diffusion coefficient, and initial gas effective diffusion coefficient are negatively correlated with the Hausdorff dimension. In general, a higher pore volume in tectonic coals results in a more even distribution of pores and greater connectivity among them, leading to a lower diffusion attenuation coefficient and enhanced gas diffusion ability. These results demonstrate that vibration can effectively improve gas desorption and diffusion in coal.

Author Contributions: Conceptualization, M.S.; methodology, M.S.; software, M.S. and W.W.; validation, M.S.; formal analysis, L.S.; investigation, Q.L.; resources, Q.L.; data curation, M.S.; writing—original draft preparation, M.S.; writing—review and editing, M.S. and P.Z.; visualization, L.S.; supervision, Z.H.; project administration, Z.H.; funding acquisition, Q.L. All authors have read and agreed to the published version of the manuscript.

Funding: This study was supported by the National Natural Science Foundation of China (52304224), the Special Project for Technology Innovation and Entrepreneurship Foundation of Tiandi Science & Technology Co., Ltd. (2021-2-TD-MS001), and the China Coal Research Institute Technology Innovation Fund (2022CX-I-05).

Data Availability Statement: The data presented in this study are available on request from the corresponding author. The data are not publicly available because they contain information that could compromise the privacy of research participants.

Conflicts of Interest: The authors declare no conflicts of interest.

References

1. Guo, Y.; Liu, X.; Li, W.; Du, F.; Ma, J.; Qian, R.; Huo, N. Research on abutment stress distribution of roof-cutting coalface: Numerical simulation and field measurement. *Geomech. Geophys. Geo-Energy Geo-Resour.* **2024**, *10*, 86. [CrossRef]
2. Wang, K.; Zhao, E.; Guo, Y.; Du, F.; Ding, K. Effect of loading rate on the mechanical and seepage characteristics of gas-bearing coal–rock and its mechanical constitutive model. *Phys. Fluids* **2024**, *36*, 026606. [CrossRef]
3. Li, J.; Hu, Q.; Yu, M.; Li, X.; Hu, J.; Yang, H. Acoustic emission monitoring technology for coal and gas outburst. *Energy Sci. Eng.* **2019**, *7*, 443–456. [CrossRef]
4. An, F.; Yuan, Y.; Chen, X.; Li, Z.; Li, L. Expansion energy of coal gas for the initiation of coal and gas outbursts. *Fuel* **2019**, *235*, 551–557. [CrossRef]
5. Guo, Y.; Wang, K.; Du, F.; Guo, H.; Li, K.; Wang, Y. Mechanical-permeability characteristics of composite coal rock under different gas pressures and damage prediction model. *Phys. Fluids* **2024**, *36*, 036615. [CrossRef]
6. Zhao, W. Diffusion Dynamics of Rapid Desorption of Gas from Pulverized Coal and Its Influence on Transporting Coal and Rock in Outbursts. Doctors' Degree, China University of Mining & Technology, Beijing, China, 2018.
7. Ren, W.; Pan, Y.; Song, S. The experimental study of the coal mass crevasse growing after coalmass vibrated with different frequency. *J. Liaoning Tech. Univ. (Nat. Sci.)* **1998**, *17*, 565–568.
8. Ren, W.; Du, G.; Pan, Y. The experimental study of rock burst prevention through vibration inducing crevasse in coal mass. *J. Fuxin Min. Inst. (Nat. Sci.)* **1997**, *16*, 687–690.
9. Pan, Y.; Du, G.; Zhang, Y.; Wang, L.; Zhang, M. Study on the mechanism of rock burst prevention by coal mass vibration. *Chin. J. Rock Mech. Eng.* **1999**, *18*, 3–5.
10. Song, Y.; Li, Z.; Cui, D. Low-frequency vibration permeability characteristics of coal and rock and analysis of loaded fracture process. *J. LiaoningTechnical Univ.* **2019**, *38*, 295–300.
11. Song, Y.; Wu, B.; Zhu, B. Study on the permeability of gas-bearing coal under mechanical vibration. *Min. Saf. Environ. Prot.* **2018**, *45*, 6–10+15.
12. Ren, Y.; Wei, J.; Wen, Z.; Zhang, J. Experimental research on influencing factors of natural frequency of coal. *China Saf. Sci. J.* **2021**, *31*, 104–111.
13. Wen, Z.; Zhang, L.; Wei, J.; Wang, J.; Zhang, J.; Jia, Y.; Ren, Y. Study on natural frequency response characteristics of coal vibration excited by simple harmonic wave. *Sci. Rep.* **2022**, *12*, 14892. [CrossRef] [PubMed]
14. Wei, J.; Zhang, J.; Wen, Z.; Zhang, L.; Ren, Y.; Si, L. Natural Frequency of Coal: Mathematical Model, Test, and Analysis on Influencing Factors. *Geofluids* **2022**, *2022*, 7891894. [CrossRef]
15. Wei, J.; Ren, Y.; Wen, Z.; Zhang, L.; Jiang, W. A New Permeability Model Under the Influence of Low-Frequency Vibration on Coal: Development and Verification. *Transp. Porous Media* **2022**, *145*, 761–787. [CrossRef]
16. Li, X.; Nie, B.; He, X. Mechanism of coal and gas bursts caused by vibration. *J. Univ. Sci. Technol. Beijing* **2011**, *33*, 149–152.
17. Shen, M.; Chen, X.; Xu, Y. Effect of Mechanical Vibration with Different Frequencies on Pore Structure and Fractal Characteristics in Lean Coal. *Shock Vib.* **2021**, *2021*, 5587592. [CrossRef]
18. Shen, M.; Chen, X. Influence rules and mechanisms of mechanical vibration at different frequencies on dynamic process of gas diffusion from coal particles. *Energy Explor. Exploit.* **2021**, *39*, 1939–1957. [CrossRef]
19. Yang, G.; Song, D.; Wang, M.; Qiu, L.; He, X.; Khan, M.; Qian, S. New insights into dynamic disaster monitoring through asynchronous deformation induced coal-gas outburst mechanism of tectonic and raw coal seams. *Energy* **2024**, *295*, 131063. [CrossRef]
20. Yan, J.; Feng, X.; Guo, Y.; Jia, T.; Tan, Z. Discussion on the Main Control Effect of Geological Structures on Coal and Gas Outburst. *ACS Omega* **2023**, *8*, 835–845. [CrossRef]
21. Wang, D.; Cheng, Y.; Yuan, L.; Wang, L.; Zhou, H. Experimental Study of Multiple Physical Properties of Tectonic Coal near a Minor Fault: Implications for Coal and Gas Outburst. *Energy Fuels* **2023**, *37*, 5878–5894. [CrossRef]

22. Tu, Q.; Cheng, Y.; Ren, T.; Wang, Z.; Lin, J.; Lei, Y. Role of Tectonic Coal in Coal and Gas Outburst Behavior During Coal Mining. *Rock Mech. Rock Eng.* **2019**, *52*, 4619–4635. [CrossRef]
23. Liu, S.; Li, X.; Li, Z.; Chen, P.; Yang, X.; Liu, Y. Energy distribution and fractal characterization of acoustic emission (AE) during coal deformation and fracturing. *Measurement* **2019**, *136*, 122–131. [CrossRef]
24. Qu, Z.; Wang, G.G.X.; Jiang, B.; Rudolph, V.; Dou, X.; Li, M. Experimental Study on the Porous Structure and Compressibility of Tectonized Coals. *Energy Fuels* **2010**, *24*, 2964–2973. [CrossRef]
25. Cheng, Y.; Pan, Z. Reservoir properties of Chinese tectonic coal: A review. *Fuel* **2020**, *260*, 116350. [CrossRef]
26. Zhang, K.; Zou, A.; Wang, L.; Cheng, Y.; Li, W.; Liu, C. Multiscale morphological and topological characterization of coal microstructure: Insights into the intrinsic structural difference between original and tectonic coals. *Fuel* **2022**, *321*, 124076. [CrossRef]
27. Wang, Z.; Cheng, Y.; Qi, Y.; Wang, R.; Wang, L.; Jiang, J. Experimental study of pore structure and fractal characteristics of pulverized intact coal and tectonic coal by low temperature nitrogen adsorption. *Powder Technol.* **2019**, *350*, 15–25. [CrossRef]
28. Guo, H.; Yu, Y.; Wang, Y.; Wang, K.; Yuan, L.; Xu, C.; Ren, B. Experimental study on the desorption law and diffusion kinetic characteristics of gas in raw coal and tectonic coal. *Energy* **2024**, *289*, 129924. [CrossRef]
29. Guo, H.; Yu, Y.; Wang, K.; Yang, Z.; Wang, L.; Xu, C. Kinetic characteristics of desorption and diffusion in raw coal and tectonic coal and their influence on coal and gas outburst. *Fuel* **2023**, *343*, 127883. [CrossRef]
30. Wang, X.; Cheng, Y.; Zhang, D.; Yang, H.; Zhou, X.; Jiang, Z. Experimental study on methane adsorption and time-dependent dynamic diffusion coefficient of intact and tectonic coals: Implications for CO_2-enhanced coalbed methane projects. *Process Saf. Environ. Prot.* **2021**, *156*, 568–580. [CrossRef]
31. Dong, J.; Cheng, Y.; Hu, B.; Hao, C.; Tu, Q.; Liu, Z. Experimental study of the mechanical properties of intact and tectonic coal via compression of a single particle. *Powder Technol.* **2018**, *325*, 412–419. [CrossRef]
32. Tu, Q.; Cheng, Y.; Xue, S.; Ren, T. Effect of particle size on gas energy release for tectonic coal during outburst process. *Fuel* **2022**, *307*, 121888. [CrossRef]
33. Lu, C.; Dou, L.; Zhang, N.; Xue, J.; Liu, G. Microseismic and acoustic emission effect on gas outburst hazard triggered by shock wave: A case study. *Nat. Hazards* **2014**, *73*, 1715–1731. [CrossRef]
34. Lu, G.; Wang, J.; Wei, C.; Song, Y.; Yan, G.; Zhang, J.; Chen, G. Pore fractal model applicability and fractal characteristics of seepage and adsorption pores in middle rank tectonic deformed coals from the Huaibei coal field. *J. Pet. Sci. Eng.* **2018**, *171*, 808–817. [CrossRef]
35. Mangi, H.N.; Detian, Y.; Hameed, N.; Ashraf, U.; Rajper, R.H. Pore structure characteristics and fractal dimension analysis of low rank coal in the Lower Indus Basin, SE Pakistan. *J. Nat. Gas Sci. Eng.* **2020**, *77*, 103231. [CrossRef]
36. Fu, H.; Tang, D.; Xu, T.; Xu, H.; Tao, S.; Li, S.; Yin, Z.; Chen, B.; Zhang, C.; Wang, L. Characteristics of pore structure and fractal dimension of low-rank coal: A case study of Lower Jurassic Xishanyao coal in the southern Junggar Basin, NW China. *Fuel* **2017**, *193*, 254–264. [CrossRef]
37. Han, W.; Zhou, G.; Gao, D.; Zhang, Z.; Wei, Z.; Wang, H.; Yang, H. Experimental analysis of the pore structure and fractal characteristics of different metamorphic coal based on mercury intrusion-nitrogen adsorption porosimetry. *Powder Technol.* **2020**, *362*, 386–398. [CrossRef]
38. Paz Ferreiro, J.; Vidal Vázquez, E. Multifractal analysis of Hg pore size distributions in soils with contrasting structural stability. *Geoderma* **2010**, *160*, 64–73. [CrossRef]
39. Wang, Z.; Wang, G.; Hao, C.; Hu, B.; Cheng, Y.; Liu, Z.; Qi, G. Study on Multifractal of Coal Pore Structure Based on Low Pressure Argon Adsorption and Its Effect on Gas Adsorption/Desorption. *Energy Fuels* **2023**, *37*, 10915–10928. [CrossRef]
40. Liu, K.; Ostadhassan, M.; Zou, J.; Gentzis, T.; Rezaee, R.; Bubach, B.; Carvajal-Ortiz, H. Multifractal analysis of gas adsorption isotherms for pore structure characterization of the Bakken Shale. *Fuel* **2018**, *219*, 296–311. [CrossRef]
41. Li, F.; Jiang, B.; Song, Y.; Cheng, G.; Lu, G. Multifractal Behavior of the Micro- and Mesopore Structures of Brittle Tectonically Deformed Coals and Its Influence on Methane Adsorption Capacity. *Energy Fuels* **2021**, *35*, 3042–3064. [CrossRef]
42. Zhang, S.; Liu, H.; Jin, Z.; Wu, C. Multifractal Analysis of Pore Structure in Middle- and High-Rank Coal by Mercury Intrusion Porosimetry and Low-Pressure N_2 Adsorption. *Nat. Resour. Res.* **2021**, *30*, 4565–4584. [CrossRef]
43. Wang, T.; Deng, Z.; Hu, H.; Wang, H.; Jiang, Z.; Wang, D. Study on the Pore Structure and Multifractal Characteristics of Medium- and High-Rank Coals Based on the Gas Adsorption Method: A Case Study of the Benxi Formation in the Eastern Margin of the Ordos Basin. *Energy Fuels* **2024**, *38*, 4102–4121. [CrossRef]
44. Li, R.; Hou, X.; Chen, L.; Fang, H.; Zheng, C. Multifractal Investigation on Multi-scale Pore Structure Heterogeneity of High Rank Coal Reservoirs. *Nat. Resour. Res.* **2022**, *31*, 1665–1685. [CrossRef]
45. Wang, D.; Hu, H.; Wang, T.; Tang, T.; Li, W.; Zhu, G.; Chen, X. Difference between of coal and shale pore structural characters based on gas adsorption experiment and multifractal analysis. *Fuel* **2024**, *371*, 132044. [CrossRef]
46. Zhang, M.; Duan, C.; Li, G.; Fu, X.; Zhong, Q.; Liu, H.; Dong, Z. Determinations of the multifractal characteristics of the pore structures of low-, middle-, and high-rank coal using high-pressure mercury injection. *J. Pet. Sci. Eng.* **2021**, *203*, 108656. [CrossRef]
47. Zhang, S.; Liu, H.; Wu, C.; Jin, Z. Influence of particle size on pore structure and multifractal characteristics in coal using low-pressure gas adsorption. *J. Pet. Sci. Eng.* **2022**, *212*, 110273. [CrossRef]

48. An, F.; Jia, H.; Wang, Z.; Liu, J.; Qi, L.; Yu, J. A model for gas diffusion in multiscale pores of coal coupling multiple diffusion mechanisms. *Energy Sources Part A Recovery Util. Environ. Eff.* **2020**, *2020*, 1–18. [CrossRef]
49. Yi, M.; Wang, L.; Liu, Q.; Hao, C.; Wang, Z.; Chu, P. Characteristics of Seepage and Diffusion in Gas Drainage and Its Application for Enhancing the gas utilization rate. *Transp. Porous Media* **2021**, *137*, 417–431. [CrossRef]
50. Li, Z.; Liu, Y.; Xu, Y.; Song, D. Gas diffusion mechanism in multi-scale pores of coal particles and new diffusion model of dynamic diffusion coefficient. *J. China Coal Soc.* **2016**, *41*, 633–643.

Disclaimer/Publisher's Note: The statements, opinions and data contained in all publications are solely those of the individual author(s) and contributor(s) and not of MDPI and/or the editor(s). MDPI and/or the editor(s) disclaim responsibility for any injury to people or property resulting from any ideas, methods, instructions or products referred to in the content.